Energy Advances

PAPER

View Article Online
View Journal | View Issue

Cite this: *Energy Adv.*, 2023, 2, 805

Atomically dispersed Co/Ni dual sites embedded in nitrogen-doped graphene for boosting oxygen evolution†

Yaoyao Deng,[a] Yao Lin,[a] Minxi Zhang,[a] Rentong Dai,[a] Zhen Luo,[a] Quanfa Zhou,[a] Mei Xiang, *[a] Jirong Bai *[a] and Shuanglong Lu *[b]

Received 3rd March 2023,
Accepted 15th April 2023

DOI: 10.1039/d3ya00099k

rsc.li/energy-advances

Exploring durable, inexpensive and high-activity electrocatalysts for efficient water oxidation is a challenge in current research. Transition metal single-atom catalysts (SACs) have been widely studied as economical electrocatalysts. However, the oxygen evolution performances of SACs are unsatisfactory because the strong bonding force between electron-donating intermediates and transition metal sites weakens the catalytic performance. Herein, atomically dispersed Co/Ni dual sites embedded in nitrogen-doped graphene (labeled as CoNi-DSA/NG) were successfully synthesized. The CoNi-DSA/NG catalyst exhibits superior oxygen evolution reaction kinetics, performance, and stability owing to the atomic dual-metal sites and their intense synergism. This study presents a prospective way to remarkably enhance the electrocatalytic performance of SACs by establishing heteronuclear dual-metal sites, and thus to expand their use into practical energy storing and converting techniques.

Introduction

The increasingly serious energy crisis and climate warming have prompted urgent exploration of clean and renewable energy. Hydrogen production from electrochemical water splitting is a promising sustainable development that can relieve the reliance on fossil energy.[1–3] The difficult part of this process is the oxygen evolution reaction (OER), a complex four-electron transfer process that results in slow kinetics. Currently, Ru/Ir catalysts are still regarded as the reference of OER electrocatalysts, but their extensive commercial application is limited by their high prices, scarcity and low stability.[4–6] Therefore, exploring cheap and earth-abundant catalysts with excellent performance toward the OER is urgently needed.

Transition metal single-atom catalysts (SACs) have aroused much attention as electrochemical catalysts owing to their effective atom utilization and high tunability of the electronic states *via* modulating the coordination environment.[7–11] Among them, carbon-supported SACs have been extensively studied because the layered structure of graphene nanosheets almost fully exposed the active centers, and thus is a perfect target for mechanism research.[12–17] Carbon-based SACs, particularly those with Fe centers (Fe SACs), perform well in the ORR.[18–20] Nevertheless, the OER abilities of SACs are unsatisfactory because the strong binding energy of electron-donating intermediates and transition metal sites decreases the catalytic behavior in the OER, which is a severe issue for the achievement of effective OER catalysis.[21,22] To strengthen the OER performance, a tactic of heteroatom doping was put forward to construct dual-single-atom (DSA) catalysts by utilizing the complementary functionalities and synergistic effect of two adjacent atomic metal species.[23–28] For example, Pei *et al.* rationally designed and prepared atomically dispersed Ni/Co dual sites anchored on N-doped carbon hollow prisms, which show excellent electrocatalytic performance toward the OER.[29] Sun *et al.* successfully synthesized atomically dispersed N-coordinated Ni–Fe dual-metal sites with higher electrocatalytic activity than mono-metal doped catalysts.[30] Wu *et al.* reported atomically dispersed Fe-Co dual metal sites (FeCo-NC) derived from Fe and Co co-doped ZIF-8, which showed excellent bifunctional catalytic activity for the ORR and OER.[31] Dual-metal sites may offer new chances for designing DSA catalysts with enhanced intrinsic activity and stability by optimizing the local geometry and electronic structure compared to traditional SACs.[32–36] However, rationally constructing DSA catalysts with high catalytic performance and clarifying their catalytic mechanisms are still challenging.

Based on the statements and information above, herein, DSA catalysts consisting of atomically dispersed Co/Ni dual sites

[a] *Research Center of Secondary Resources and Environment, School of Chemical Engineering and Materials, Changzhou Institute of Technology, Changzhou 213032, China. E-mail: xiangm@czu.cn, baijr@czu.cn*

[b] *Key Laboratory of Synthetic and Biological Colloids, Ministry of Education, School of Chemical and Material Engineering, Jiangnan University, Wuxi, Jiangsu 214122, P. R. China. E-mail: lushuanglong@jiangnan.edu.cn*

† Electronic supplementary information (ESI) available. See DOI: https://doi.org/10.1039/d3ya00099k

anchored on nitrogen-doped graphene (labeled as CoNi-DSA/NG) were rationally designed and synthesized by pyrolyzing cobalt acetate, nickel acetate, L-alanine and melamine together in an argon (Ar) atmosphere. Thanks to the numerous dual-metal active sites and the cooperative effect from Co–Ni atomic pairs, CoNi-DSA/NG exhibits extraordinary OER activity with an overpotential of 214 mV at 10 mA cm^{-2}, and a Tafel slope of only 81 mV dec^{-1}, which are much better than those of Co-SA/NG and Ni-SA/NG.[37] In addition, the stability of CoNi-DSA/NG was evaluated by multi-cycle cyclic voltammetry (CV) curves, and the overpotential only rose by 11 mV at 10 mA cm^{-2} after 3000 cycles. This study provides a prospective strategy to rationally design the DSA catalysts and to significantly enhance the electrocatalytic ability of SACs.

Experimental section

Chemicals and materials

Cobalt acetate tetrahydrate ($Co(CH_3COO)_2{\cdot}4H_2O$), nickel acetate tetrahydrate ($Ni(CH_3COO)_2{\cdot}4H_2O$), ethanol (99.7%) (all AR), L-alanine, melamine, and hydrochloric acid (HCl 36.0–38.0%) (both CP) were all made by Sinopharm Chemical Reagent Co., Ltd. All reagents were used as received.

Preparation of CoNi-DSA/NG

Firstly, 2 g of melamine, 2 g of L-alanine, 25 mg of $Co(CH_3COO)_2{\cdot}4H_2O$ and 25 mg of $Ni(CH_3COO)_2{\cdot}4H_2O$ were homogeneously mixed by grinding. Then, 15 mL of ethanol and 3 mL of HCl were added, and the slurry was stirred on a magnetic stirrer until the ethanol evaporated completely. The resulting solids were dried in a vacuum oven at 60 °C for 24 h and then ground again for 30 minutes. The obtained powder was pyrolyzed in a tube furnace in an Ar atmosphere, heated to 900 °C at a rate of 3 °C min^{-1}, and held at this temperature for 2 h. The sample as-obtained was soaked in 3 M HCl to discard metal grains, and then washed with water several times until the supernatant was neutral. The black precipitates were oven-dried under vacuum into a black power, and annealed at 900 °C for 1 h in Ar to form CoNi-DSA/NG.

Results and discussion

The preparation process of atomically dispersed Co/Ni dual sites anchored on nitrogen-doped graphene (CoNi-DSA/NG) was implemented by a two-step pyrolysis strategy, as exhibited in Scheme 1. Firstly, cobalt acetate, nickel acetate, L-alanine and melamine were mixed uniformly and then pyrolyzed at 900 °C for 2 h under an Ar atmosphere, in which melamine and L-alanine were *in situ* decomposed and evolved into nitrogen-doped graphene that can anchor Co and Ni atoms.[38] The black power was cleaned with a 3 M HCl solution to remove unstable metal grains, and then re-annealed at 900 °C for 1 h in Ar to restore the crystallinity, forming a CoNi-DSA/NG catalyst with highly-dispersed Co/Ni dual sites. We also synthesized atomically dispersed Co or Ni single atom sites anchored on nitrogen-doped graphene (marked as Co-SA/NG or Ni-SA/NG, respectively) using the same method.

Transmission electron microscopy (TEM) images of CoNi-DSA/NG, Co-SA/NG and Ni-SA/NG exhibit the morphology of graphene-like carbon sheets (Fig. 1a, b and Fig. S1, ESI†). The TEM images show no evident metal grains, implying the existence of atomically dispersed Co/Ni active sites. The high-resolution TEM (HRTEM) of CoNi-DSA/NG shows the lattice fringes of graphitic carbon, without obvious metal lattice fringes (Fig. 1c). Therefore, we utilized the aberration-corrected high-angle annular dark-field scanning TEM (AC-HAADF-STEM) to explore the existing forms of Co and Ni in CoNi-DSA/NG. The high-density bright spots in the AC-HAADF-STEM image reveal the distribution of Co and Ni sites in the CoNi-DSA/NG (Fig. 1d). Abundant atomic pairs can be observed (partially circled by the red dashed lines), suggesting that Co/Ni dual-metal sites may be generated. Besides, the metal contents of CoNi-DSA/NG, Co-DSA/NG and Ni-DSA/NG were detected using inductively coupled plasma optical emission spectrometry (ICP-OES) (Table S1, ESI†). The total metal content in CoNi-DSA/NG is approximately double those of Co-SA/NG and Ni-SA/NG. The larger metal-loading capacity of CoNi-DSA/NG may be ascribed to the Co and Ni interaction for mutual stabilization.

For an exploration of the distributions of Co, Ni, N and C, element mapping was used to investigate the CoNi-DSA/NG.

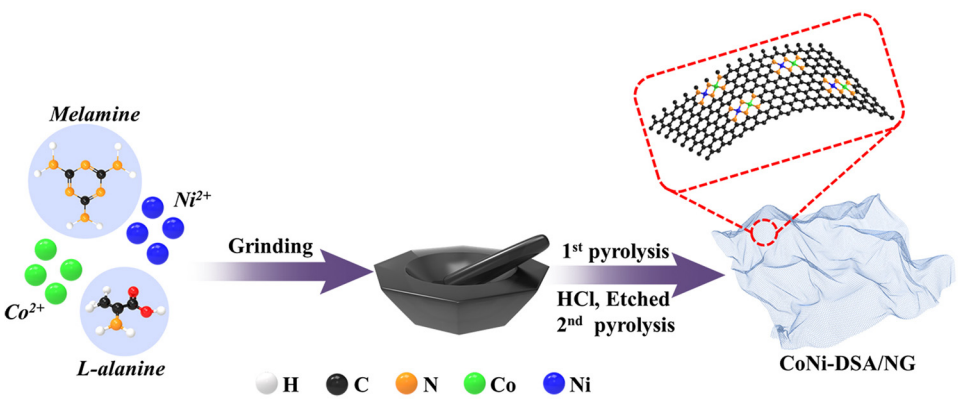

Scheme 1 Schematic preparation of CoNi-DSA/NG.

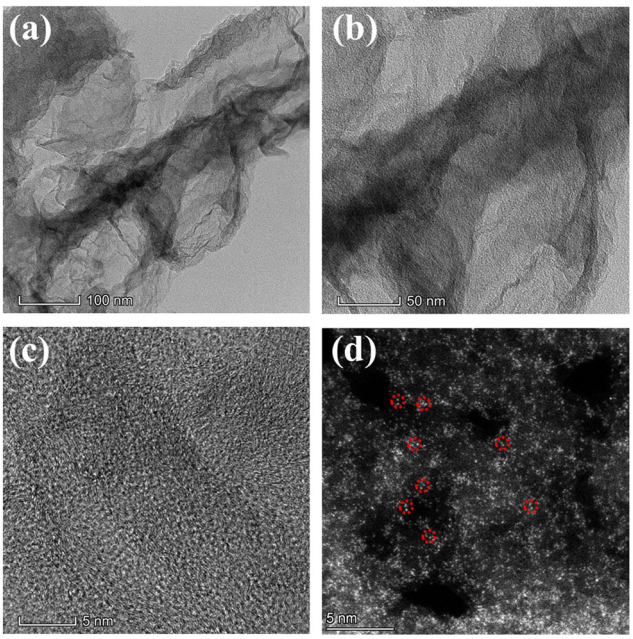

Fig. 1 (a and b) TEM, (c) HRTEM, and (d) AC-HAADF-STEM images of CoNi-DSA/NG.

The HAADF-STEM further reveals that CoNi-DSA/NG has a sheet structure and no obvious metal particles (Fig. 2a). Accordingly, the elemental mapping of CoNi-DSA/NG exhibits that the atomically dispersed Co and Ni both are evenly spread throughout the nitrogen-doped graphene nanosheets (Fig. 2b–f). The presence of both Co and Ni signals proves the successful embedding of diatomic sites into nitrogen-doped graphene.

The phase states and structures of the samples were characterized by X-ray diffraction (XRD). The XRD patterns of CoNi-DSA/NG, Co-SA/NG and Ni-SA/NG all show an intense peak at $\sim 26^{\circ}$ and a slight peak at $\sim 44^{\circ}$, which are in accordance with the (002) and (101) planes of graphitic carbon, respectively (Fig. 3a). Moreover, the XRD patterns of all three catalysts show no peak related to metal or metal compounds, which implies the absence of any metal grain.[39] Raman spectra can well uncover the orderly or disorderly crystal structures of carbon materials. The Raman spectrum of CoNi-DSA/NG contains a characteristic G band at 1590 cm^{-1} and a D band at 1362 cm^{-1} (Fig. 2b), which match with graphitic carbon (G band) and disordered carbon (D band), respectively.[40,41] In addition, the N_2 adsorption/desorption assays were conducted to test the specific surface areas and porosity of CoNi-DSA/NG, Co-SA/NG and Ni-SA/NG. The Brunauer–Emmett–Teller (BET) specific surface areas of CoNi-DSA/NG, Co-SA/NG and Ni-SA/NG are 404.61, 330.56, and 304.35 $m^2\ g^{-1}$, respectively (Fig. 2c). The CoNi-DSA/NG, Co-SA/NG and Ni-SA/NG are mainly mesoporous (about 3–4 nm), which facilitates electrolyte penetration and the exposure of the active sites (Fig. 2d).[42]

The elemental composition and valence state of the CoNi-DSA/NG were studied *via* X-ray photoelectron spectroscopy (XPS). The high-resolution C 1s spectrum of CoNi-DSA/NG in Fig. 4a is fitted into three peaks at 284.8 (C–C), 285.7 (C–N) and 288.2 (C–O) eV.[43] The high-resolution N 1s spectrum shows an obvious metal–N peak ($\sim$399.2 eV), suggesting that the metal–N bonds mainly coordinate the metal sites fixed on carbon (Fig. 4b). The metal–N bonds will cause metal–N interactions, which is pivotal in the stabilization and catalytic behavior of single atoms. Besides, the N 1s spectrum also comprises

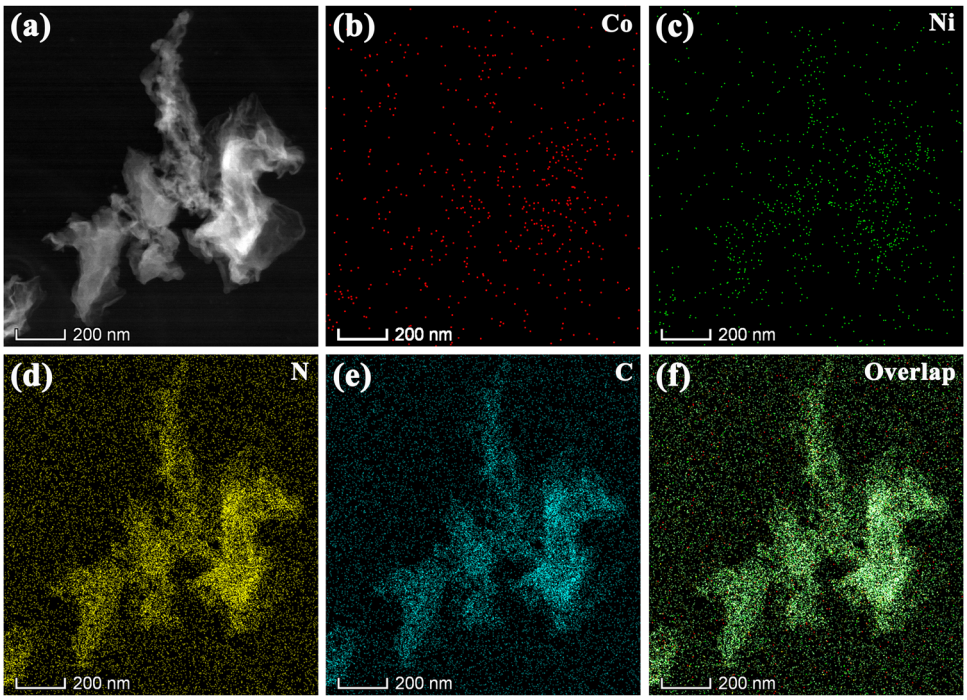

Fig. 2 (a) HAADF-STEM image, EDX elemental mapping of (b) Co, (c) Ni, (d) N and (e) C, and (f) overlap of CoNi-DSA/NG.

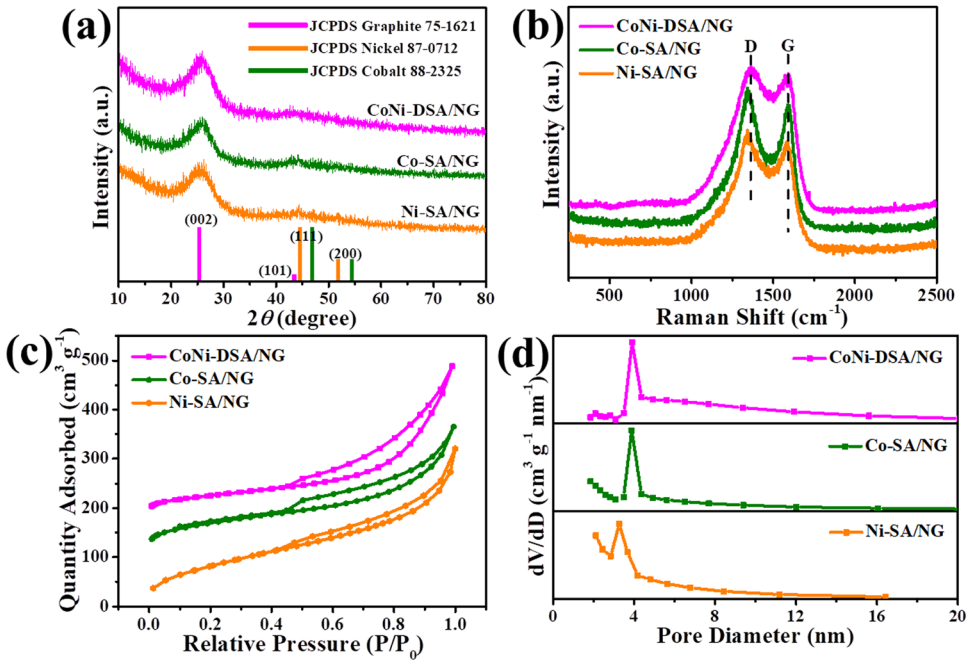

Fig. 3 (a) XRD patterns, (b) Raman spectra, (c) N_2 adsorption/desorption isotherms, and (d) the homologous pore distribution of CoNi-DSA/NG, Co-SA/NG and Ni-SA/NG.

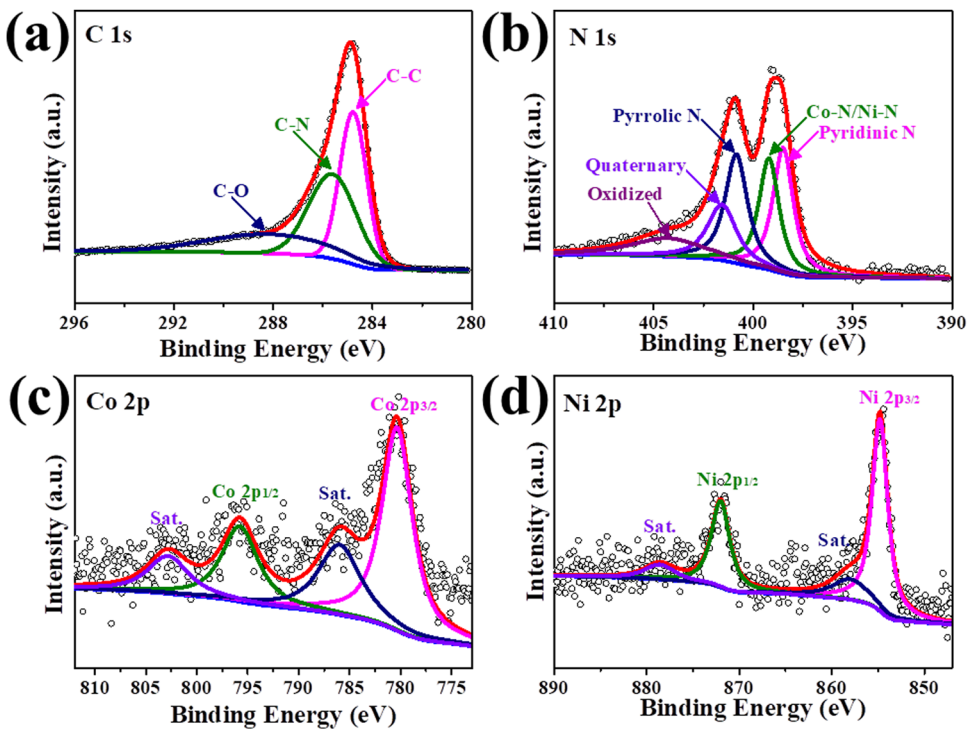

Fig. 4 XPS survey spectra of (a) C1s, (b) N 1s, (c) Co 2p, and (d) Ni 2p of CoNi-DSA/NG.

pyridinic N (398.5 eV), pyrrolic N (400.9 eV), quaternary (401.6 eV), and oxidized (404.3 eV) N species, respectively.[29,44] Co 2p and Ni 2p of CoNi-DSA/NG uncover one chemical state between zero and divalent of Co and Ni (780.4, 795.9, 854.8 and 872.1 eV for Co $2p_{3/2}$, Co $2p_{1/2}$, Ni $2p_{3/2}$ and Ni $2p_{1/2}$, respectively, Fig. 4c and d) together with two wide satellite peaks, which is in line with the reported valence of SACs.[45,46] These results demonstrate that the CoNi-DSA/NG is well synthesized

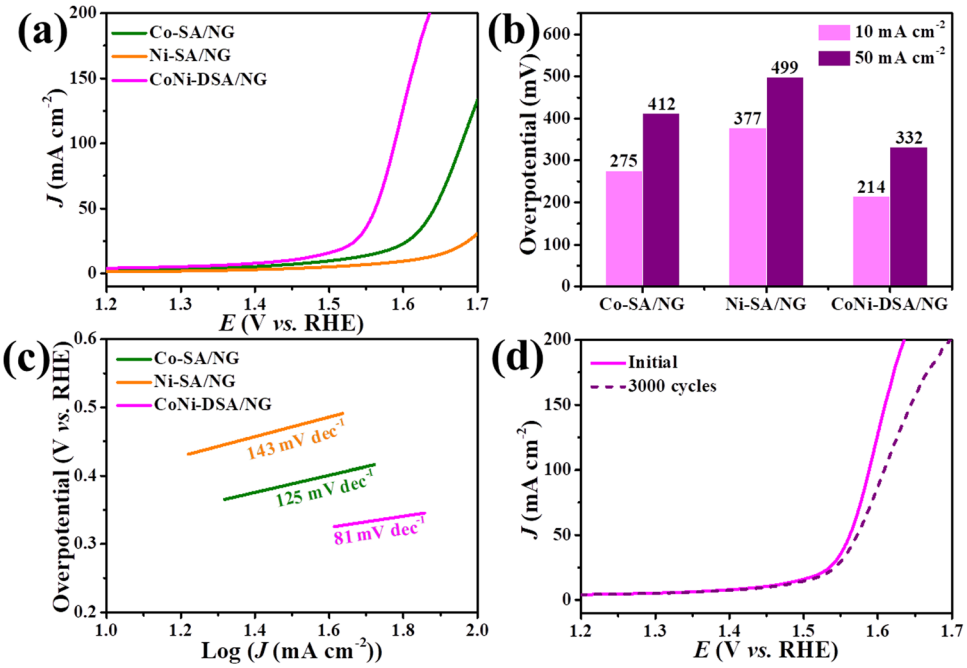

Fig. 5 (a) OER polarization curves, (b) overpotential contrast at the current density of 10 and 50 mA cm^{-2}, and (c) Tafel slopes of Co-SA/NG, Ni-SA/NG and CoNi-DSA/NG. (d) The polarization curves before and after 3000 CV of CoNi-DSA/NG (all tested in 1.0 M KOH solution).

and is a prospective OER electrocatalyst with abundant metal-N active sites.

To assess the electrochemical behaviors of the catalysts, we utilized a representative three-electrode system to measure the OER performances of CoNi-DSA/NG, Co-SA/NG and Ni-SA/NG in a 1.0 M KOH solution. Fig. 5a exhibits the *iR*-compensated linear scan voltammetry (LSV) curves, in which CoNi-DSA/NG shows continually the largest current density in the whole potential range. Obviously, CoNi-DSA/NG requires the lowest overpotential of 214 and 332 mV at the current densities of 10 and 50 mA cm^{-2}, respectively (Fig. 5b), which surpass those of Co-SA/NG (274 and 412 mV), Ni-SA/NG (377 and 499 mV) and some of the reported catalysts in the literature (Table S2, ESI†). The above results demonstrate that CoNi-DSA/NG possesses higher catalytic activity than Co-SA/NG and Ni-SA/NG, which may be attributed to the catalytic synergism between Co and Ni atoms.[47,48] Moreover, to explore the catalytic kinetics, the Tafel slopes of catalysts were plotted by linearly fitting the polarization curves. The Tafel slope of CoNi-DSA/NG is 81 mV dec^{-1} (Fig. 5c), which is lower than those of Co-SA/NG (125 mV dec^{-1}) and Ni-SA/NG (143 mV dec^{-1}). This result indicates that CoNi-DSA/NG possesses a faster OER rate in alkaline solutions.[49] Additionally, the stability of CoNi-DSA/NG was tested by multi-cycle CV (Fig. 5d). Comparing the LSV of this catalyst before and after 3000 CV, the overpotential only rose by 11 mV at 10 mA cm^{-2}. Those results demonstrate that CoNi-DSA/NG has superior electrocatalytic effectiveness and stability in the OER under alkaline conditions.

To explore the reasons for the superior catalytic activity of CoNi-DSA/NG, the electrochemical double-layer capacitance (C_{dl}) was detected using cyclic voltammetry (CV) at varying scan rates in a non-faradaic zone, which can reflect the electrochemical active surface area (ECSA) (Fig. S2, ESI†).[50] CoNi-DSA/NG possesses a C_{dl} of 4.4 mF cm^{-2}, significantly larger than those

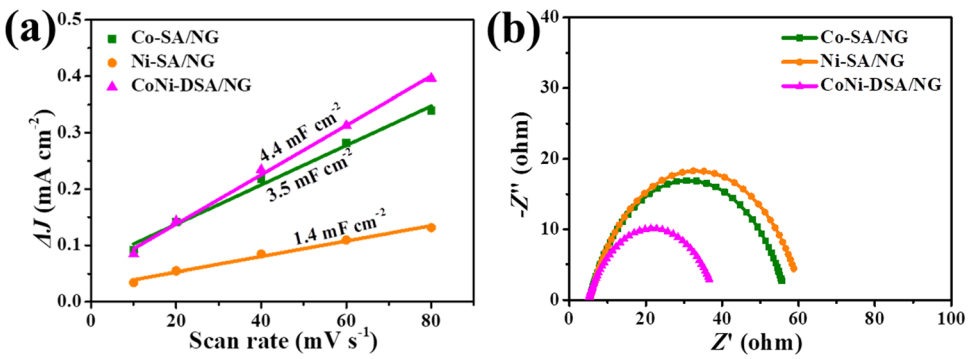

Fig. 6 (a) The plots of charging current density differences of the catalysts against scan rates. (b) EIS plots at 1.62 V *vs.* RHE.

of Co-SA/NG and Ni-SA/NG (3.5 and 1.4 mF cm^{-2} respectively; Fig. 6a), indicating that CoNi-DSA/NG has larger ECSA. Moreover, electrochemical impedance spectroscopy (EIS) implies that CoNi-DSA/NG has the smallest charge transfer resistance, which well accords with the lowest Tafel slope.[30,51] In all, the considerably better catalytic activity and kinetic procedure of CoNi-DSA/NG fully verify the synergism of Co/Ni dual sites on enhancing the OER performance.

Conclusions

We successfully synthesized atomically-dispersed Co and Ni bimetal sites fixed in nitrogen-doped graphene (CoNi-DSA/NG). Electrochemical measurements demonstrate that the CoNi-DSA/NG catalyst exhibits superior OER kinetics, activity and stability because of the excellent design and strong synergism of atomic dual-metal sites. This study offers an outstanding method to remarkably enhance the electrocatalytic behaviors of single-atom catalysts by building heteronuclear dual-metal sites and thus contributes to their extensive use in practical energy storing and converting techniques.

Conflicts of interest

There are no conflicts to declare.

Acknowledgements

This work was funded by the Natural Science Foundation of the Jiangsu Higher Education Institutions of China (20KJB150044, 20KJB430038, 20KJB530006), and the National Natural Science Foundation of China (No. 22208032).

References

1 M. Wang, K. Sun, W. Mi, C. Feng, Z. Guan, Y. Liu and Y. Pan, Interfacial Water Activation by Single-Atom Co-N_3 Sites Coupled with Encapsulated Co Nanocrystals for Accelerating Electrocatalytic Hydrogen Evolution, *ACS Catal.*, 2022, **12**, 10771–10780.
2 Q. Zhang and J. Guan, Atomically dispersed catalysts for hydrogen/oxygen evolution reactions and overall water splitting, *J. Power Sources*, 2020, **471**, 228446.
3 L. Li, D. Yu, P. Li, H. Huang, D. Xie, C.-C. Lin, F. Hu, H.-Y. Chen and S. Peng, Interfacial electronic coupling of ultrathin transition-metal hydroxide nanosheets with layered MXenes as a new prototype for platinum-like hydrogen evolution, *Energy Environ. Sci.*, 2021, **14**, 6419–6427.
4 X. Han, X. Ling, D. Yu, D. Xie, L. Li, S. Peng, C. Zhong, N. Zhao, Y. Deng and W. Hu, Atomically Dispersed Binary Co–Ni Sites in Nitrogen-Doped Hollow Carbon Nanocubes for Reversible Oxygen Reduction and Evolution, *Adv. Mater.*, 2019, **31**, 1905622.
5 C. Rong, X. Shen, Y. Wang, L. Thomsen, T. Zhao, Y. Li, X. Lu, R. Amal and C. Zhao, Electronic Structure Engineering of Single-Atom Ru Sites via Co-N_4 Sites for Bifunctional pH-universal Water Splitting, *Adv. Mater.*, 2022, **34**, 2110103.
6 Q. Wang, Z. Zhang, C. Cai, M. Wang, Z. L. Zhao, M. Li, X. Huang, S. Han, H. Zhou, Z. Feng, L. Li, J. Li, H. Xu, J. S. Francisco and M. Gu, Single Iridium Atom Doped Ni_2P Catalyst for Optimal Oxygen Evolution, *J. Am. Chem. Soc.*, 2021, **143**, 13605–13615.
7 Y. Zhao, X. F. Lu, G. Fan, D. Luan, X. Gu and X. W. Lou, Surface-Exposed Single-Ni Atoms with Potential-Driven Dynamic Behaviors for Highly Efficient Electrocatalytic Oxygen Evolution, *Angew. Chem., Int. Ed.*, 2022, 202212542.
8 H. Shang, W. Sun, R. Sui, J. Pei, L. Zheng, J. Dong, Z. Jiang, D. Zhou, Z. Zhuang, W. Chen, J. Zhang, D. Wang and Y. Li, Engineering Isolated Mn-N_2C_2 Atomic Interface Sites for Efficient Bifunctional Oxygen Reduction and Evolution Reaction, *Nano Lett.*, 2020, **20**, 5443–5450.
9 C.-X. Zhao, J.-N. Liu, J. Wang, C. Wang, X. Guo, X.-Y. Li, X. Chen, L. Song, B.-Q. Li and Q. Zhang, A clicking confinement strategy to fabricate transition metal single-atom sites for bifunctional oxygen electrocatalysis, *Sci. Adv.*, 2022, **8**, eabn5091.
10 Z. Zhang, X. Zhao, S. Xi, L. Zhang, Z. Chen, Z. Zeng, M. Huang, H. Yang, B. Liu, S. J. Pennycook and P. Chen, Atomically Dispersed Cobalt Trifunctional Electrocatalysts with Tailored Coordination Environment for Flexible Rechargeable Zn-Air Battery and Self-Driven Water Splitting, *Adv. Energy Mater.*, 2020, **10**, 2002896.
11 F. Luo, J. Zhu, S. Ma, M. Li, R. Xu, Q. Zhang, Z. Yang, K. Qu, W. Cai and Z. Chen, Regulated coordination environment of Ni single atom catalyst toward high-efficiency oxygen electrocatalysis for rechargeable Zinc-air batteries, *Energy Storage Mater.*, 2021, **35**, 723–730.
12 Y. Shang, X. Duan, S. Wang, Q. Yue, B. Gao and X. Xu, Carbon-based single atom catalyst: Synthesis, characterization, DFT calculations, *Chin. Chem. Lett.*, 2022, **33**, 663–673.
13 W. Wan, Y. Zhao, S. Wei, C. A. Triana, J. Li, A. Arcifa, C. S. Allen, R. Cao and G. R. Patzke, Mechanistic insight into the active centers of single/dual-atom Ni/Fe-based oxygen electrocatalysts, *Nat. Commun.*, 2021, **12**, 5589.
14 J. Ban, X. Wen, H. Xu, Z. Wang, X. Liu, G. Cao, G. Shao and J. Hu, Dual Evolution in Defect and Morphology of Single-Atom Dispersed Carbon Based Oxygen Electrocatalyst, *Adv. Funct. Mater.*, 2021, **31**, 2010472.
15 Q. Zhang and J. Guan, Single-Atom Catalysts for Electrocatalytic Applications, *Adv. Funct. Mater.*, 2020, **30**, 2000768.
16 F. Chang, Y. Ma, P. Su and J. Liu, Synthesis of a graphitized hierarchical porous carbon material supported with a transition metal for electrochemical conversion, *Inorg. Chem. Front.*, 2022, **9**, 1794–1801.
17 W. Li, Y. Wu, M. Chen, P. Dai, T. Jiang and S. Zhou, Ultrathin nitrogen-doped defective carbon layer embedded with NiFe for solid zinc-air batteries, *J. Alloys Compd.*, 2022, **925**, 166658.
18 W. Cheng, P. Yuan, Z. Lv, Y. Guo, Y. Qiao, X. Xue, X. Liu, W. Bai, K. Wang, Q. Xu and J. Zhang, Boosting Defective Carbon by Anchoring Well-Defined Atomically Dispersed

Metal-N_4 Sites for ORR, OER, and Zn-Air Batteries, *Appl. Catal., B*, 2020, **260**, 118198.

19 J. Sheng, S. Sun, G. Jia, S. Zhu and Y. Li, Doping Effect on Mesoporous Carbon-Supported Single-Site Bifunctional Catalyst for Zinc-Air Batteries, *ACS Nano*, 2022, **16**(10), 15994–16002.

20 Y. Yan, H. Cheng, Z. Qu, R. Yu, F. Liu, Q. Ma, S. Zhao, H. Hu, Y. Cheng, C. Yang, Z. Li, X. Wang, S. Hao, Y. Chen and M. Liu, Recent progress on the synthesis and oxygen reduction applications of Fe-based single-atom and double-atom catalysts, *J. Mater. Chem. A*, 2021, **9**, 19489–19507.

21 H. Fei, J. Dong, Y. Feng, C. S. Allen, C. Wan, B. Volosskiy, M. Li, Z. Zhao, Y. Wang, H. Sun, P. An, W. Chen, Z. Guo, C. Lee, D. Chen, I. Shakir, M. Liu, T. Hu, Y. Li, A. I. Kirkland, X. Duan and Y. Huang, General synthesis and definitive structural identification of MN_4C_4 single-atom catalysts with tunable electrocatalytic activities, *Nat. Catal.*, 2018, **1**, 63–72.

22 Z. Zeng, L. Y. Gan, H. B. Yang, X. Su, J. Gao, W. Liu, H. Matsumoto, J. Gong, J. Zhang, W. Cai, Z. Zhang, Y. Yan, B. Liu and P. Chen, Orbital coupling of hetero-diatomic nickel-iron site for bifunctional electrocatalysis of CO_2 reduction and oxygen evolution, *Nat. Commun.*, 2021, **12**, 4088.

23 T. Cui, Y.-P. Wang, T. Ye, J. Wu, Z. Chen, J. Li, Y. Lei, D. Wang and Y. Li, Engineering Dual Single-Atom Sites on 2D Ultrathin N-doped Carbon Nanosheets Attaining Ultra-Low-Temperature Zinc-Air Battery, *Angew. Chem., Int. Ed.*, 2022, **61**, 202115219.

24 R. Li and D. Wang, Superiority of Dual-Atom Catalysts in Electrocatalysis: One Step Further Than Single-Atom Catalysts, *Adv. Energy Mater.*, 2022, **12**, 2103564.

25 W. Zhang, Y. Chao, W. Zhang, J. Zhou, F. Lv, K. Wang, F. Lin, H. Luo, J. Li, M. Tong, E. Wang and S. Guo, Emerging Dual-Atomic-Site Catalysts for Efficient Energy Catalysis, *Adv. Mater.*, 2021, **33**, 2102576.

26 H. Liu, H. Rong and J. Zhang, Synergetic Dual-Atom Catalysts: The Next Boom of Atomic Catalysts, *ChemSusChem*, 2022, **15**, 202200498.

27 Y. Zhou, L. Chen, L. Sheng, Q. Luo, W. Zhang and J. Yang, Dual-metal atoms embedded into two-dimensional covalent organic framework as efficient electrocatalysts for oxygen evolution reaction: A DFT study, *Nano Res.*, 2022, **15**, 7994–8000.

28 Q. An, J. Jiang, W. Cheng, H. Su, Y. Jiang and Q. Liu, Recent Advances in Dual-Atom Site Catalysts for Efficient Oxygen and Carbon Dioxide Electrocatalysis, *Small Methods*, 2022, **6**, 2200408.

29 Z. Pei, X. F. Lu, H. Zhang, Y. Li, D. Luan and X. W. Lou, Highly Efficient Electrocatalytic Oxygen Evolution Over Atomically Dispersed Synergistic Ni/Co Dual Sites, *Angew. Chem., Int. Ed.*, 2022, 202207537.

30 C. Wu, X. Zhang, Z. Xia, M. Shu, H. Li, X. Xu, R. Si, A. I. Rykov, J. Wang, S. Yu, S. Wang and G. Sun, Insight into the role of Ni–Fe dual sites in the oxygen evolution reaction based on atomically metal-doped polymeric carbon nitride, *J. Mater. Chem. A*, 2019, **7**, 14001–14010.

31 Y. He, X. Yang, Y. Li, L. Liu, S. Guo, C. Shu, F. Liu, Y. Liu, Q. Tan and G. Wu, Atomically Dispersed Fe-Co Dual Metal Sites as Bifunctional Oxygen Electrocatalysts for Rechargeable and Flexible Zn-Air Batteries, *ACS Catal.*, 2022, **12**, 1216–1227.

32 D. Yu, Y. Ma, F. Hu, C. C. Lin, L. Li, H. Y. Chen, X. Han and S. Peng, Dual-Sites Coordination Engineering of Single Atom Catalysts for Flexible Metal-Air Batteries, *Adv. Energy Mater.*, 2021, **11**, 2101242.

33 H. Liu, X. Xu, H. Xu, S. Wang, Z. Niu, Q. Jia, L. Yang, R. Cao, L. Zheng and D. Cao, Dual active site tandem catalysis of metal hydroxyl oxides and single atoms for boosting oxygen evolution reaction, *Appl. Catal., B*, 2021, **297**, 120451.

34 R. Hu, Y. Li, Q. Zeng and J. Shang, Role of active sites in N-coordinated Fe-Co dual-metal doped graphene for oxygen reduction and evolution reactions: A theoretical insight, *Appl. Surf. Sci.*, 2020, **525**, 146588.

35 C. Zhang, S. Qin, B. Li and P. Jin, Dual-metal atom incorporated N-doped graphenes as oxygen evolution reaction electrocatalysts: high activities achieved by site synergies, *J. Mater. Chem. A*, 2022, **10**, 8309–8323.

36 T. He, A. R. P. Santiago, Y. Kong, M. A. Ahsan, R. Luque, A. Du and H. Pan, Atomically Dispersed Heteronuclear Dual-Atom Catalysts: A New Rising Star in Atomic Catalysis, *Small*, 2022, **18**, 2106091.

37 B. Hu, A. Huang, X. Zhang, Z. Chen, R. Tu, W. Zhu, Z. Zhuang, C. Chen, Q. Peng and Y. Li, Atomic Co/Ni dual sites with N/P-coordination as bifunctional oxygen electrocatalyst for rechargeable zinc-air batteries, *Nano Res.*, 2021, **14**, 3482–3488.

38 M. Zhang, H. Li, J. Chen, L. Yi, P. Shao, C.-Y. Xu and Z. Wen, Nitrogen-doped graphite encapsulating RuCo nanoparticles toward high-activity catalysis of water oxidation and reduction, *Chem. Eng. J.*, 2021, **422**, 130077.

39 Y. Cheng, S. He, J. P. Veder, R. De Marco, S. Z. Yang and S. Ping Jiang, Atomically Dispersed Bimetallic FeNi Catalysts as Highly Efficient Bifunctional Catalysts for Reversible Oxygen Evolution and Oxygen Reduction Reactions, *ChemElectroChem*, 2019, **6**, 3478–3487.

40 Z. Li, H. He, H. Cao, S. Sun, W. Diao, D. Gao, P. Lu, S. Zhang, Z. Guo, M. Li, R. Liu, D. Ren, C. Liu, Y. Zhang, Z. Yang, J. Jiang and G. Zhang, Atomic Co/Ni dual sites and Co/Ni alloy nanoparticles in N-doped porous Janus-like carbon frameworks for bifunctional oxygen electrocatalysis, *Appl. Catal., B*, 2019, **240**, 112–121.

41 L. Li, Y. Ma, F. Cui, Y. Li, D. Yu, X. Lian, Y. Hu, H. Li and S. Peng, Novel Insight into Rechargeable Aluminum Batteries with Promising Selenium Sulfide@Carbon Nanofibers Cathode, *Adv. Mater.*, 2023, **35**, 2209628.

42 X. Zhang, Y. Li, M. Jiang, J. Wei, X. Ding, C. Zhu, H. He, H. Lai and J. Shi, Engineering the coordination environment in atomic Fe/Ni dual-sites for efficient oxygen electrocatalysis in Zn-air and Mg-air batteries, *Chem. Eng. J.*, 2021, **426**, 130758.

43 K. Khan, X. Yan, Q. Yu, S.-H. Bae, J. J. White, J. Liu, T. Liu, C. Sun, J. Kim, H.-M. Cheng, Y. Wang, B. Liu, K. Amine, X. Pan and Z. Luo, Stone-Wales defect-rich carbon-supported dual-metal single atom sites for Zn-air batteries, *Nano Energy*, 2021, **90**, 106488.

44 X. Zhou, J. Gao, Y. Hu, Z. Jin, K. Hu, K. M. Reddy, Q. Yuan, X. Lin and H. J. Qiu, Theoretically Revealed and Experimentally Demonstrated Synergistic Electronic Interaction of CoFe Dual-Metal Sites on N-doped Carbon for Boosting Both Oxygen Reduction and Evolution Reactions, *Nano Lett.*, 2022, **22**, 3392–3399.

45 F. Wang, T. Feng, X. Jin, Y. Zhou, Y. Xu, Y. Gao, H. Li and J. Lei, Atomic Co/Ni active sites assisted MOF-derived rich nitrogen-doped carbon hollow nanocages for enhanced lithium storage, *Chem. Eng. J.*, 2021, **420**, 127583.

46 L. Wang, Y. Hao, L. Deng, F. Hu, S. Zhao, L. Li and S. Peng, Rapid complete reconfiguration induced actual active species for industrial hydrogen evolution reaction, *Nat. Commun.*, 2022, **13**, 5785.

47 Y. Ma, H. Fan, C. Wu, M. Zhang, J. Yu, L. Song, K. Li and J. He, An efficient dual-metal single-atom catalyst for bifunctional catalysis in zinc-air batteries, *Carbon*, 2021, **185**, 526–535.

48 Y. Hao, D. Yu, S. Zhu, C.-H. Kuo, Y.-M. Chang, L. Wang, H.-Y. Chen, M. Shao and S. Peng, Methanol upgrading coupled with hydrogen product at large current density promoted by strong interfacial interactions, *Energy Environ. Sci.*, 2023, **16**, 1100–1110.

49 L. Wang, L. Song, Z. Yang, Y. M. Chang, F. Hu, L. Li, L. Li, H. Y. Chen and S. Peng, Electronic Modulation of Metal–Organic Frameworks by Interfacial Bridging for Efficient pH-Universal Hydrogen Evolution, *Adv. Funct. Mater.*, 2022, **33**, 2210322.

50 C. Han, W. Yi, S. Feng, Z. Li and H. Song, Single-atom palladium anchored N-doped carbon towards oxygen electrocatalysis for rechargeable Zn-air batteries, *Dalton Trans.*, 2022, **51**, 12314–12323.

51 G. Liu, B. Wang, P. Ding, W. Wei, Y. Ye, L. Wang, W. Zhu, H. Li and J. Xia, In-situ synthesis strategy for CoM (M = Fe, Ni, Cu) bimetallic nanoparticles decorated N-doped 1D carbon nanotubes/3D porous carbon for electrocatalytic oxygen evolution reaction, *J. Alloys Compd.*, 2020, **815**, 152470.